35th Annual International Conference of the IEEE EMBS
Osaka, Japan, 3 - 7 July, 2013

COMPUTATIONAL MODEL OF CEREBELLAR TRANSCRANIAL DIRECT CURRENT STIMULATION

M. Parazzini, E. Rossi, R. Ferrucci, S. Fiocchi, I. Liorni, A. Priori, P. Ravazzani

Abstract — **This work aimed to estimate the distribution of the electric field and current density generated by cerebellar tDCS using electromagnetics computational techniques applied to a realistic human models of different ages and gender.**

Results show that the stronger electric field and current density occur mainly in the cerebellar cortex, with a spread toward the occipital region of the cortex, while the current spread to other structures is negligible. Moreover, changes of about 1 cm in the position of the scalp electrode delivering tDCS did not influence the E and J distribution in the cerebellum.

I. Introduction

Transcranial Direct Current Stimulation (tDCS) is a non-invasive technique that modulates brain excitability [1-3]. Recently tDCS over the cerebellum (or cerebellar tDCS)has been used to modulate motor and cognitive brain circuits [4-7]. Notwithstanding its clinical use, there are still open questions on cerebellar tDCS. One of these is the amount and the spread of the electrical current that crosses the skull and reaches the cerebellum.

The aim of this work is to evaluate the electric field (**E**) and the current density (**J**) of cerebellar tDCS by using computational electromagnetic techniques on realistic human models, allowing to analyze current flow through the brain, and the cerebellum. This could be of some help not only for better understanding the actual mechanism of cerebellar tDCS but also in the investigation about the possible involvement of the cerebral cortex during cerebellar stimulation. Moreover, this study could provide answer to possible concerns about the safety of this tDCS application, providing some information about the levels of the fields in sensitive areas such as the brainstem and the heart.

II. Material and Methods

Simulations were conducted using the simulation platform SEMCAD X (by SPEAG, www.speag.com), solving the Laplace equation to determine the electric potential (φ) distribution inside the human tissues.

M. Parazzini, S. Fiocchi, I. Liorni and P. Ravazzani are with Istituto di Ingegneria Biomedica ISIB-CNR, Milano 20133 Italy (corresponding author: marta.parazzini@polimi.it; serena.fiocchi@polimi.it, ilaria.liorni@polimi.it and paolo.ravazzani@polimi.it).

E. Rossi. and I. Liorni are also with Dipartimento di Elettronica, Informazione e Bioingegneria DEIB, Politecnico di Milano, Milano 20133 Italy (elena.rossi@newronika.it).

R. Ferrucci and A. Priori are with Dipartimento di Fisiopatologia Medico-Chirurgica e dei Trapianti, Università degli Studi di Milano, Milano, Italy and with Centro Clinico per la Neurostimolazione, le Neurotecnologie ed i Disordini del Movimento, Fondazione IRCCS Ca' Granda Ospedale Maggiore Policlinico, Milano, Italy (roberta.ferrucci@policlinico.mi.it; alberto.priori@unimi.it)

$$\nabla\cdot(\sigma\nabla\varphi)=0 \qquad (1)$$

where σ is the electrical conductivity of the human tissues. The **E** and **J** field distributions were obtained by means of the following relations:

$$\mathbf{E}=-\nabla\varphi \qquad (2)$$

$$\mathbf{J}=\sigma\mathbf{E} \qquad (3)$$

The realistic human models of the Virtual Family [8] were used. i) a 26-years-old female adult model "Ella"; ii) a 34 years-old male adult model "Duke"; iii) a 11 years old female adolescent model "Billie". All the models were in a voxel-based format at a resolution of 1 mm and consisted of up to 77 different tissues, the dielectric properties of which were assigned on the basis of the literature data at low frequency [9-10], following an approach already used in literature [11-12].

The active electrode was placed on the scalp over the cerebellum area (about 2 cm under the inion, 1 cm posterior to the mastoid process) and the reference over the right arm as reported in clinical applications [4-5]. The electrodes were modeled as rectangular pads conductors (σ =5.9x107 S/m) of 5x7 cm^2 placed above a rectangular sponge (σ = 0.3 S/m) of 7x8 cm^2. The potential difference between the electrodes was adjusted to inject a total current of 2 mA. Fig. 1 shows a view of the electrodes positioning during cerebellar tDCS.

The spatial amplitude distributions of **E** and **J** were analyzed in different brain regions, such as the cerebellum, the cortex, the white matter, the medulla oblongata, the pons, the midbrain, and the thalamus. Moreover, since the reference electrode is placed extra-cephalic on the right arms, these distributions were also evaluated in the heart. To assess if the **E** and **J** field are influenced by the exact electrode placement, the active electrode was moved longitudinally and laterally of ± 0.5 cm for the model "Ella".

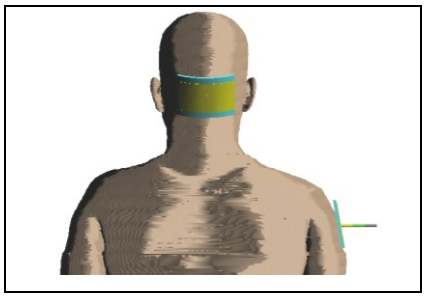

Figure 1. Back view of the electrodes positioning for the model "Ella".

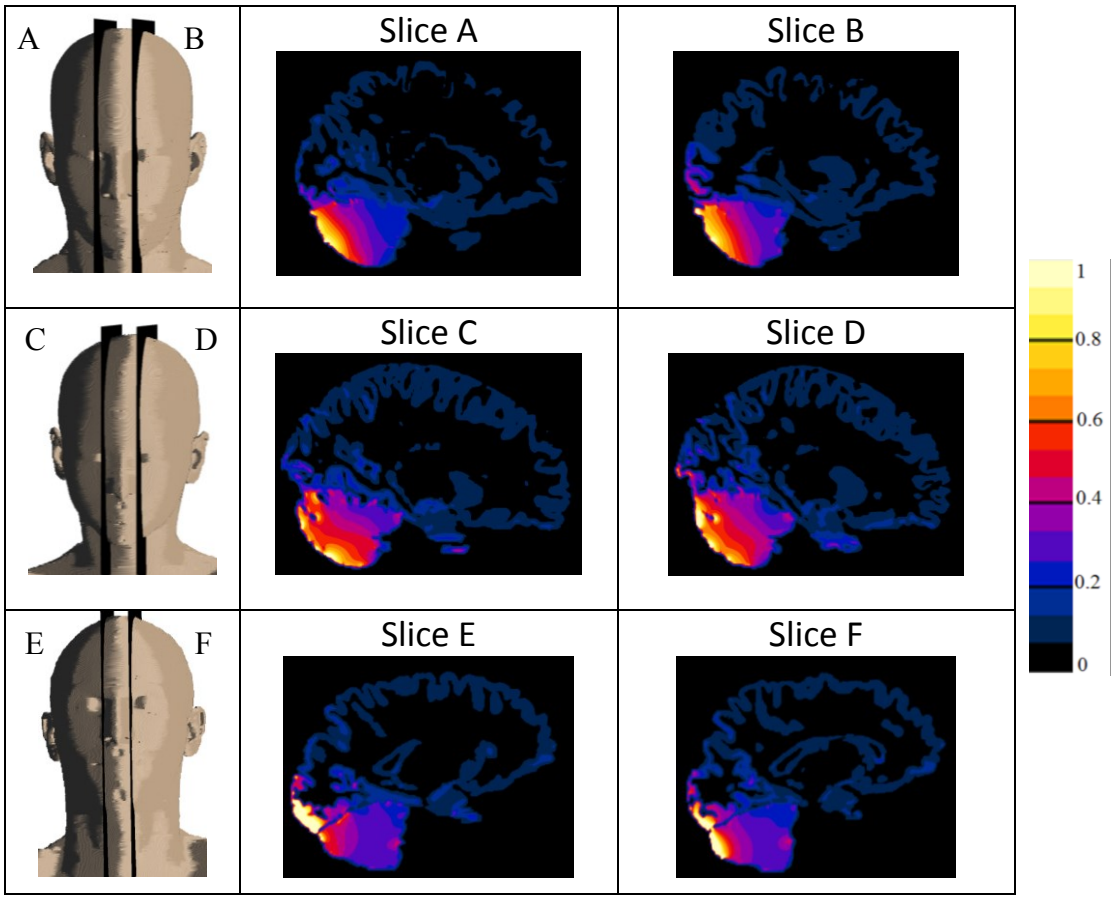

Figure 2. Parasagittal sections of the current density amplitude distribution on the cortex and on the cerebellum for the model "Ella" (top row), "Billie" (middle row) and "Duke" (bottom row), respectively.

III. Results

Fig. 2 shows parasagittal brain sections of the **J** amplitude distribution on the cortex and on the cerebellum for the model "Ella" (top row), "Billie" (middle row) and "Duke" (bottom row), respectively. All the other tissues have been masked of the images to allow comparison of the distributions in these two tissues only. The values are normalized with respect to the maximum of the **J**-field amplitude in the cerebellum.

These panels clearly show that the higher **J**-field amplitudes generated by cerebellar tDCS were below the active electrode in the cerebellum at cortical level within the posterior lobe, with a spread toward the occipital region of the cortex. This spread has been quantified as the percentage of volume of the occipital cortex where the amplitude of **J**-field is greater than 70% of the peak of **J** found in the cerebellum. It results in a maximum of 4% for the "Duke" model, while it is much less than 1% for the other two models.

Interestingly, the figure shows also that, particularly in the adolescent "Billie", the **J**-field amplitude distribution is more widespread toward the more anterior part of the cerebellum. Indeed, whereas the percentage of volume of the cerebellum where the amplitude of **J**-field is greater than 70% of its peak was comparable with the one obtained in the adult models, the percentage of volume where the amplitude of **J**-field is greater than 50% of its peak is 2.5 times higher than that in the adult models and was 27.2%.

To give a concise but quantitative estimate of these distributions at the level of specific brain regions of interest, Fig. 3 shows the average across the human models of the descriptive statistics of **E** (top panel) and **J** (bottom panel) field distributions evaluated in the cerebellum, the occipital cortex, the white matter, the medulla oblongata, the pons, the midbrain, and the thalamus. Both these graphs noticeably show that both peak and median values of **E** and **J** were higher in the cerebellum.

Data in the figure show that apart from the occipital cortex, the **E** and **J** field distributions marginally spread also to other brain structures. In particular, compared to the values found in the cerebellum, the medians of **E** and **J** in the other brain structures are reduced from 44% to 78% and from 68% to 87%, across the different structures, for **E** and **J**, respectively. Furthermore, the values found in the pons and the midbrain agree with our previous estimation [13] showing that tDCS with an extracephalic reference electrode is not relevant at the level of the brainstem.

The spatial distribution of both **E** and **J** were also estimated at the level of the heart muscle to evaluate the

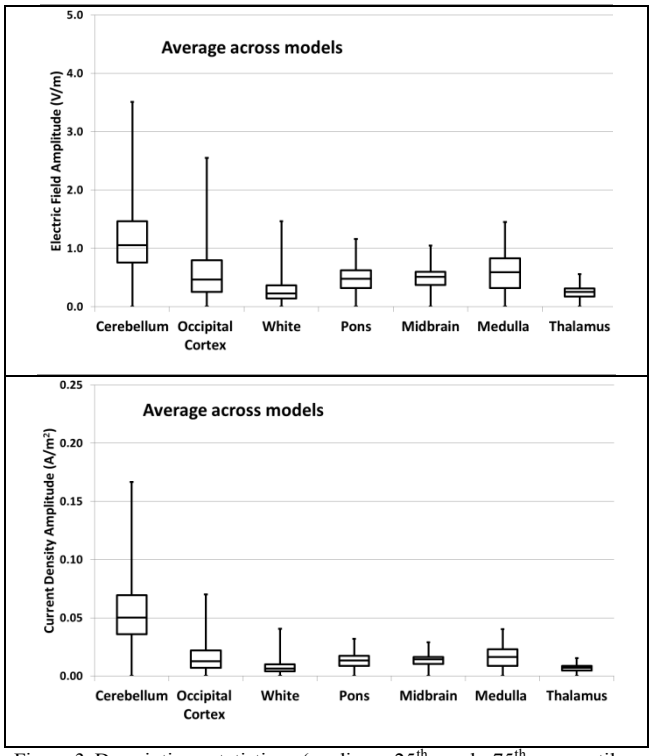

Figure 3 Descriptive statistics (median, 25th and 75th percentiles, minimum and 99th percentile) of electric field (top) and current density (bottom) amplitude distribution in different brain tissues averaged across the three human models.

cardiac safety during cerebellar tDCS. The average across the human models of the peaks of these distributions are 0.66 V/m and 0.04 A/m^2. Both these values are in good agreement with published modeling data [14] where the cardiac safety of the use of an extra-cephalic reference electrode on the right arms for a tDCS at 2 mA has been discussed.

Finally, small changes in the placement of the active electrode resulted in a small effect on the field amplitude distributions. In particular, the **J** spread over the occipital cortex remains always less than 1%, as before for the same human model. Moreover, changing the electrode position, the maximum difference among the percentage of volume of the cerebellum where the amplitude of **J**-field is greater than 70% of its peak is less than 1% (with the higher value when the active electrode is moved laterally to the right), while the maximum difference among the percentage of volume where the amplitude of **J**-field is greater than 50% of its peak is about 2%, with the higher spread toward the more anterior part of the cerebellum when the active electrode is moved longitudinally toward the anion.

IV. Discussions and Conclusions

Despite some inter-individual differences, our modeling study confirms that the cerebellum is the only structure to be significantly involved by cerebellar tDCS. Indeed cerebellar tDCS generates the highest **E** and **J** below the stimulating electrode in the posterior cerebellum with a small spread to other structures. Within the cerebellum the current density distribution varied across different subjects, being maximum toward the more anterior part in the youngest model "Billie". This observation could be particularly useful in the clinical application of cerebellar tDCS in children and adolescents.

Modeling approach reveals also that the current spreading to other anatomical structures outside the cerebellum is unlike to produce functional effects. This conclusion is in line with previous clinical observations that cerebellar tDCS failed to influence visual evoked potentials excluding, therefore, a direct stimulation of the visual cortex [4].

Interestingly, the **E** and **J** spreads to the brainstem and the heart were negligible, thus further supporting the safety of this technique.

Small changes in the active electrode position results in a slight effect on the field amplitude distributions. This suggests that fine placement of the stimulating electrode does not influence so much the current density in the cerebellum and in the occipital cortex. Therefore, sophisticated neuronavigation systems are not specifically required for cerebellar tDCS, further supporting the simplicity and easy applicability of the technique.

Our results show that individual anatomical variability somehow influences the field distribution. For example, the "Duke" model is characterized by higher spread of the field amplitude toward the occipital region of the cortex compared to the other models. The spread could be explained by different cerebrospinal fluid distribution and/or skull thickness [15]. Therefore, even if the distributions are quite similar among the models, individual anatomical features should be considered in future studies and the modeling approach we used might be relevant for clinical applications of cerebellar tDCS to customize and optimize the treatment.

References

[1] A. Priori, "Brain polarization in humans: A reappraisal of an old tool for prolonged non-invasive modulation of brain excitability", *Clin. Neurophysiol*, vol. 114, no. 4, pp. 589-95, 2003.

[2] M.A. Nitsche, W. Paulus, "Transcranial direct current stimulation-update 2011", *Restor Neurol Neurosci,* vol. 29, pp.463-92, 2011.

[3] A.R. Brunoni, M.A. Nitsche, N. Bolognini, M. Bikson, T. Wagner, L. Merabet, D.J. Edwards, A. Valero-Cabre, A. Rotenberg, A. Pascual-Leone, R. Ferrucci, A. Priori, P.S. Boggio, F. Fregni, "Clinical research with transcranial direct current stimulation (tDCS): Challenges and future directions", *Brain Stimul,*vol. 5, no. 3, pp. 175-95, 2012.

[4] R. Ferrucci, S. Marceglia, M. Vergari, F. Cogiamanian, S. Mrakic-Sposta, F. Mameli, S. Zago, S. Barbieri, A. Priori, "Cerebellar transcranial direct current stimulation impairs the practice-dependent proficiency increase in working memory", *J Cogn Neurosci*, vol. 20, no.9, pp 1687-97, 2008.

[5] R. Ferrucci, G. Giannicola, M. Rosa, M. Fumagalli, P.S. Boggio, M. Hallett, S. Zago, A. Priori, "Cerebellum and processing of negative facial emotions: Cerebellar transcranial DC stimulation specifically enhances the emotional recognition of facial anger and sadness", *Cogn Emot,* vol. 26, no.5, pp. 786-99, 2012.

[6] G. Jayaram, B. Tang, R. Pallegadda, E.V. Vasudevan, P. Celnik, A. Bastian, “Modulating locomotor adaptation with cerebellar stimulation”, *J Neurophysiol,* vol. 107, no. 11, 2950-7, 2012.
[7] J.M. Galea, G. Jayaram, L. Ajagbe, P. Celnik, “Modulation of cerebellar excitability by polarity-specific noninvasive direct current stimulation”, *J Neurosci,* vol. 29, no. 28, pp. 9115-22, 2009.
[8] A. Christ, W. Kainz, G.E. Hahn, et al., “The Virtual Family-development of surface-based anatomical models of two adults and two children for dosimetric simulations,” *Phys Med Biol*; vol. 55, pp. N23-N38, 2010.
[9] S. Gabriel, R.W. Lau, C. Gabriel, “The dielectric properties of biological tissues: II. Measurements in the frequency range 10 Hz to 20 GHz,” *Phys Med Biol,* vol. 41, no. 11, pp. 2251-2269,1996.
[10] National Research Council, Institute for Applied Physics "Nello Carrara", IFAC-CNR, Florence, Italy. An Internet resource for the calculation of the dielectric properties of body tissues. Published at http://niremf.ifac.cnr.it/tissprop/ (last accessed on January 9, 2013).
[11] M. Parazzini, S. Fiocchi, E. Rossi, A. Paglialonga, P. Ravazzani, “Transcranial Direct Current Stimulation: Estimation of the Electric Field and of the Current Density in an Anatomical Human Head Model,” *IEEE Trans Biomed Eng*, vol. 58, no. 6, pp. 1773-1780, 2011.
[12] M. Parazzini, S. Fiocchi, P. Ravazzani, “Electric field and current density distribution in an anatomical head model during transcranial direct current stimulation for tinnitus treatment,” *Bioelectromagnetics,* 2012, 33(6): 476-487
[13] M. Parazzini, E. Rossi, L. Rossi, A. Priori, P. Ravazzani, “Evaluation of the current density in the brainstem during transcranial direct current stimulation with extra-cephalic reference electrode”, *Clin Neurophysiol.* 2012 [Epub ahead of print].
[14] M. Parazzini, E. Rossi, L. Rossi, A. Priori, Ravazzani P., “Numerical estimation of the current density in the heart during transcranial direct current stimulation”, *Brain Stimul* 2012 [Epub ahead of print].
[15] M. Bikson, A. Rahman, A. Datta, F. Fregni, L. Merabet, “High-resolution modeling assisted design of customized and individualized transcranial direct current stimulation protocols”, *Neuromodulation*, vol. 15, no. 4, pp. 306-15, 2012;